

Side illumination fluorescence emission characteristics from a dye doped polymer optical fiber under two-photon excitation

M. Sheeba,^{1,*} M. Rajesh,³ S. Mathew,² V. P. N. Nampoori,¹
C. P. G. Vallabhan,² and P. Radhakrishnan¹

¹International School of Photonics, Cochin University of Science and Technology, Cochin 682 022 India

²Center of Excellence in Lasers and Optoelectronic Sciences, Cochin University of Science and Technology, Cochin 682 022, India

³School of Engineering and Mathematical Sciences, City University London, Northampton Square, London EC1V 0HB, UK

*Corresponding author: sheebanambiar@gmail.com

Received 3 December 2007; revised 8 February 2008; accepted 13 February 2008;
posted 13 February 2008 (Doc. ID 90429); published 7 April 2008

Two-photon excited (TPE) side illumination fluorescence studies in a Rh6G–RhB dye mixture doped polymer optical fiber (POF) and the effect of energy transfer on the attenuation coefficient is reported. The dye doped POF is pumped sideways using 800 nm, 70 fs laser pulses from a Ti:sapphire laser, and the TPE fluorescence emission is collected from the end of the fiber for different propagation distances. The fluorescence intensity of RhB doped POF is enhanced in the presence of Rh6G as a result of energy transfer from Rh6G to RhB. Because of the reabsorption and reemission process in dye molecules, an effective energy transfer is observed from the shorter wavelength part of the fluorescence spectrum to the longer wavelength part as the propagation distance is increased in dye doped POF. An energy transfer coefficient is found to be higher at shorter propagation distances compared to longer distances. A TPE fluorescence signal is used to characterize the optical attenuation coefficient in dye doped POF. The attenuation coefficient decreases at longer propagation distances due to the reabsorption and reemission process taking place within the dye doped fiber as the propagation distance is increased. © 2008 Optical Society of America

OCIS codes: 060.2270, 060.2280, 060.2400, 060.7140, 060.4370, 060.2300.

1. Introduction

Polymer optical fibers (POFs) have attracted much attention during the past two decades because of their unique characteristics, such as flexibility, ease in handling, and relatively low cost in coupling [1–3]. With the development of POFs, increasing research activities have also been carried out in the field of amplifiers and lasers in POF and waveguides [4–9]. Two-photon excited (TPE) frequency upconversion lasing and two-photon fluorescence imaging have also been a subject of intensive research in recent years [10–12].

Multiphoton transitions involving the simultaneous absorption of more than one photon were first predicted by Goppert–Mayer in 1931 [13] and were demonstrated in the laboratory in 1961 by Kaiser and Garrett [14].

Compact, lightweight, and inexpensive lasers operating in the short wavelength visible region are desired for use in such diverse applications as medical diagnostics, surgery, high-capacity optical storage, and high-resolution scanning and printing. Methods for generating these shorter wavelengths include optical harmonic generation and sum frequency mixing techniques that require phase matching in expensive inorganic crystals. An excellent alternative to generate these shorter wavelengths is the frequency

upconversion of two-photon absorption (TPA) by pumping in the infrared.

There have been two important technical approaches to achieve frequency upconversion lasing: (1) simultaneous absorption of two photons by the gain medium (two-photon pumped) [15–20] and (2) sequential stepwise multiphoton excitation (multistep one-photon pumped) [21,22]. Considering that the TPE cross section is much smaller than the corresponding one-photon cross section, a higher pump intensity and longer gain length are required for TPE lasing purposes. Advantages of using waveguide or fiber configurations to achieve upconversion lasing are (1) a higher local pump intensity and (2) a much longer effective gain length. Upconversion lasing in a dye doped polymer waveguide and a dye doped polymer fiber have been reported [19,20].

We report the TPE fluorescence studies in a Rhodamine(Rh)6G, RhB, and Rh6G–RhB dye mixture doped POF. Our studies illustrate that the combination of a well-designed mixture of organic chromophores incorporated into a fiber geometry is appealing for the development of an upconversion polymer fiber laser that can be tunable over a broader wavelength region. The optical attenuation in a POF is an important parameter of interest, and for the successful fabrication of an upconversion dye doped polymer fiber laser, frequency upconverted emission and the propagation loss mechanisms in the dye doped POF should be studied.

Usually the propagation loss in fibers and planar waveguide structures is measured by the cutback technique, where the transmitted signal is measured at the end of the fiber as a function of length. The disadvantage of the cutback technique is that it is a destructive method [23,24]. A nondestructive side illumination fluorescence (SIF) technique for measuring the optical attenuation in dye doped fibers has been developed by Kruhlak and Kuzyk [25,26]. We describe the use of this technique to investigate the TPE fluorescence emission, energy transfer process, and its effect on the attenuation coefficient in single dye and dye mixture doped POF.

2. Experiment

The dye doped POFs used for the studies in this paper are based on polymethyl methacrylate (PMMA), which was chosen as the host as it has good optical quality and is compatible with most of the organic dyes used as dopants. The dyes used as dopants are Rh6G and RhB, which have a high quantum yield, low intersystem crossing rate, low excited state absorption at both pump and lasing wavelengths, and reasonably good photostability. The dye doped POF for this paper is fabricated as described in our previous paper [27]. To investigate the energy transfer process and its effect on the attenuation coefficient in a dye doped POF, four fiber samples with a diameter of 400 μm are used having the following dye concentrations: (a) Rh6G (0.25 mM), (b) Rh6G (0.25 mM) and RhB (0.11 mM), (c) Rh6G (0.25 mM) and RhB (0.25 mM), and (d) RhB

(0.25 mM). Absorption and fluorescence emission spectra of samples are recorded using a standard spectrophotometer and spectrofluorimeter, respectively.

A schematic of the experimental setup for the TPE SIF studies from a dye doped POF is shown in Fig. 1. A mode-locked Ti:sapphire laser (Tsunami, Spectra Physics, USA) is used as the pump source, which has an output wavelength of 800 nm, a pulse width of 70 fs, and an average power of 0.4 W at a repetition rate of 80 MHz. The fiber is mounted normally onto a translation stage with respect to the incident beam. The pump beam is focused on the fiber using a convex lens of an appropriate focal length. When the femtosecond laser pulse is focused, very high peak power is produced at the focal volume leading to simultaneous absorption of two photons. It can be noted that although there is no linear absorption for dyes Rh6G and RhB in the range of 800–1100 nm, the two-photon energy within the range of 800–1100 nm falls just within the linear absorption band (400–550 nm) of these dyes (Fig. 2) and can lead to TPA. Xu and Webb have reported that the TPE peak wavelength appears blueshifted relative to twice the one-photon absorption (OPA) peak wavelength in the case of Rh dyes, and the TPE peak wavelength is observed to be ~ 800 nm [28]. Therefore our choice of an 800 nm pump source is the best for recording the TPE fluorescence spectrum in the case of Rh dyes, but it is to be noted here that, in the case of a PMMA based POF, absorption due to C–H vibrations is a big source of attenuation in this wavelength region that needs to be reduced to make low loss waveguides.

The side illumination of the dye doped fiber generates a TPE fluorescence emission at the focal point. Light emission is collected from one end of the dye doped fiber using a collecting optical fiber coupled to a monochromator–CCD system (Acton Spectropro). To measure the transmitted fluorescence as a function of the propagation distance through the fiber, the illumination point on the fiber is varied by translating the fiber horizontally across the laser source.

3. Results and Discussion

Two types of energy transfer processes that figure in our investigations are discussed in Subsections 3.A and 3.B.

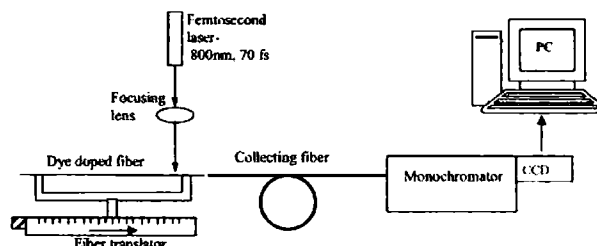


Fig. 1. Experimental setup to record the TPE SIF emission from the dye doped POF.

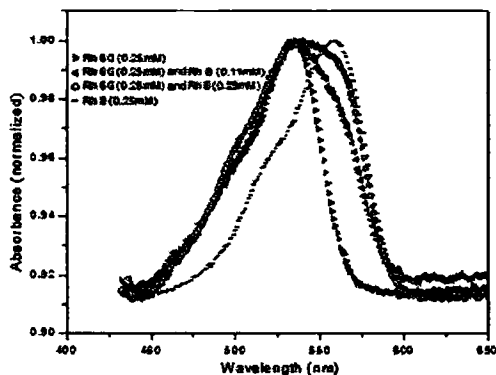


Fig. 2. Absorption spectra of Rh6G, RhB, and dye mixture doped PMMA samples.

A. Case 1

The first one is the energy transfer occurring from the dye Rh6G to RhB. There is a strong overlap between the emission spectrum of Rh6G and the absorption spectrum of RhB as shown in Fig. 3, which clearly indicates the possibility of energy transfer from Rh6G to RhB. A nonradiative type fluorescence resonance energy transfer (FRET) has been reported for a Rh6G–RhB dye mixture system [29,30].

To have an idea about the nonradiative type FRET in the Rh6G–RhB dye mixture system, the Forster distance R_0 is evaluated using the equation [31–34]

$$(R_0)^6 = \frac{9000 \ln 10 K^2 \phi_d}{128 \pi^5 N n^4} \int F_D(\lambda) \epsilon_A(\lambda) \lambda^4 d\lambda, \quad (1)$$

where R_0 , known as the Forster distance, is the characteristic distance between the donor and the acceptor molecule at which the energy transfer efficiency is 50%, ϕ_d is the quantum yield of the donor in the absence of the acceptor, which is taken as 0.75 in the case of Rh6G in the PMMA matrix [35], n is the refractive index of the medium, which is taken

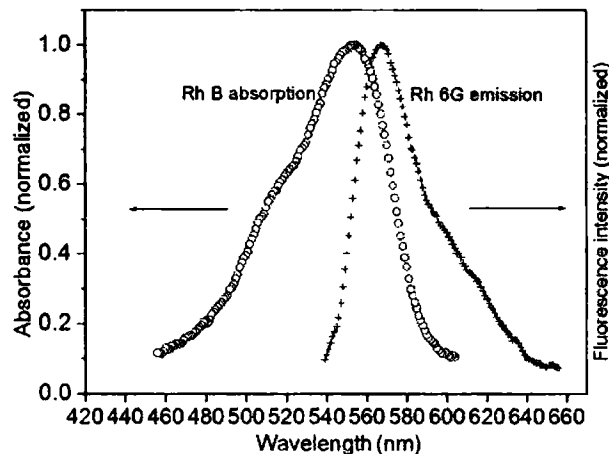


Fig. 3. Spectral overlap between the absorption of the RhB (0.25 mM) doped PMMA and the emission of the Rh6G (0.25 mM) doped PMMA samples.

as 1.49 for PMMA [36], N is Avogadro's number, and k^2 is the orientation factor of two dipoles interacting and is usually assumed to be equal to two-thirds for isotropic media [31]. $F_D(\lambda)$ is the corrected fluorescence intensity of the donor in the wavelength range λ to $\lambda + \Delta\lambda$ with the total intensity normalized to unity. $\epsilon_A(\lambda)$ is the extinction coefficient of the acceptor at λ , which is in units of $M^{-1}cm^{-1}$.

The overlap integral,

$$J(\lambda) = \int F_D(\lambda) \epsilon_A(\lambda) \lambda^4 d\lambda, \quad (2)$$

expresses the degree of spectral overlap between the donor emission and the acceptor absorption and is calculated using the MATLAB program.

Thus from Eq. (1), R_0 is evaluated to be 55 Å, which is within the limit of 10–90 Å in which FRET can be possible [30,31,37–39]. So it can be inferred that the nonradiative FRET can be a possible mechanism in the Rh6G–RhB dye mixture system along with the radiative type energy transfer in the present case. FRET occurs as a result of the long range dipole-dipole Coulomb interaction between the donor and the acceptor molecules.

Figure 4 shows a comparison of the TPE SIF emission from the POF doped with Rh6G, Rh6G–RhB dye mixture system, and RhB. The propagation distance of the transmitted fluorescence emission through the fiber is 26 mm. In the case of the Rh6G (0.25 mM) doped POF, the fluorescence emission peak is observed to be at 591 nm [Fig. 4(a)]. Consider the case of the Rh6G (0.25 mM) and RhB (0.11 mM) doped POF [Fig. 4(b)], it is to be noted that both the Rh6G and the RhB dyes can get excited by TPA and exhibit their own fluorescence in the dye mixture system since the quantum yield of fluorescence is almost equal for both dyes. As a result of the strong overlap between the Rh6G emission and the RhB absorption,

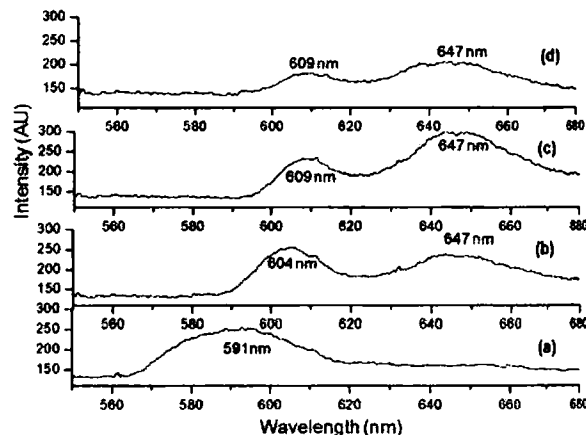


Fig. 4. Shift of fluorescence emission peak as a result of the energy transfer process in a dye mixture doped POF (a) Rh6G (0.25 mM), (b) dye mixture Rh6G (0.25 mM) and RhB (0.11 mM), (c) dye mixture Rh6G (0.25 mM) and RhB (0.25 mM), and (d) RhB (0.25 mM).

energy transfer occurs from Rh6G to RhB through radiative (shorter wavelength part of the fluorescence emission of the Rh6G gets reabsorbed and reemitted by the RhB molecules) and nonradiative (FRET) paths. Thus, in Fig. 4(b) the fluorescence spectrum peak is observed to be redshifted to 604 nm because of the energy transfer from Rh6G to RhB. Also a second peak is observed at 647 nm, which is the characteristic peak from RhB. In the case of a Rh6G (0.25 mM) and RhB (0.25 mM) doped POF [Fig. 4(c)], the first peak in the fluorescence emission is shifted more to the red side at 609 nm. In this case the energy transfer from Rh6G to RhB is maximum, and the spectrum looks the same as that of a RhB (0.25 mM) doped POF [Fig. 4(d)]. This is due to the fact that a maximum energy transfer occurs when both dyes are taken in equal concentration [40]. Figure 4(d) represents the fluorescence spectrum corresponding to RhB (0.25 mM) alone.

Again, consider the fluorescence intensity of the three samples in Figs 4(b)–4(d). Compared to the RhB (0.25 mM) doped sample, the fluorescence intensity (for example, at 647 nm) is slightly more than in the case of the Rh6G (0.25 mM) and RhB (0.11 mM) doped mixture sample as a result of the energy transfer from Rh6G to RhB. For the Rh6G (0.25 mM) and RhB (0.25 mM) doped sample, the fluorescence intensity is enhanced more than that of the samples in Figs 4(b) and 4(d) because of the maximum energy transfer in this case. Table 1 summarizes the observations from above.

B. Case 2

There is an overlap between the absorption and the fluorescence emission from the dye molecules as shown in Fig. 5. Thus, as the propagation distance increases, the propagating fluorescence light gets self-absorbed and reemitted at a longer wavelength causing a redshift in the emitted fluorescence spectrum [41,42]. In effect, this self-absorption re emission process causes a radiative energy transfer from the shorter wavelength part of the fluorescence spectrum to the longer wavelength part as the propagation distance is increased. The effect of this energy transfer on the attenuation coefficient will be discussed in detail in Subsection 3.C.

Figure 6 shows the TPE SIF spectra for different propagation distances (4–26 mm) through the fiber in the case of the above-mentioned four samples (a) Rh6G (0.25 mM), (b) Rh6G (0.25 mM) and RhB (0.11 mM), (c) Rh6G (0.25 mM) and RhB (0.25 mM),

Table 1. Enhancement in RhB Fluorescence Intensity as a Result of the Energy Transfer from Rh6G to RhB

Concentration of Samples	Fluorescence Intensity of RhB (at 647 nm) A.U.
RhB (0.25 mM)	200
Rh6G (0.25 mM) and RhB (0.11 mM)	231
Rh6G (0.25 mM) and RhB (0.25 mM)	293

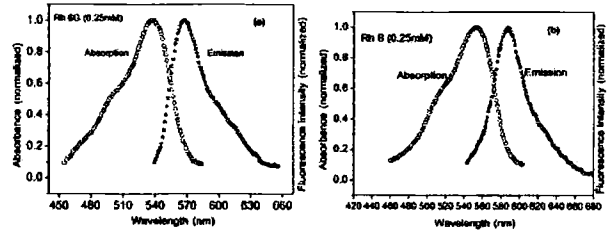


Fig. 5. Spectral overlap between the absorption and the emission spectra of dye doped samples (a) Rh6G (0.25 mM) doped PMMA and (b) RhB (0.25 mM) doped PMMA.

and (d) RhB (0.25 mM). Three important observations can be deduced from these plots.

1. As the propagation distance increases, the overall magnitude of the fluorescence intensity decreases in all the cases due to loss mechanisms such as absorption and scattering of the fluorescence emission.

2. There is a redshift for the peak fluorescence emission in all four cases as the illumination distance from the collecting end of the fiber is increased.

Figure 7 shows the variation of the peak fluorescence emission with the propagation distance through the fiber for the four samples. A clear redshift in the peak fluorescence emission wavelength is observed for the first peak as the propagation distance is increased from 4 to 26 mm. This redshift is 581.5–592.1 nm in the case of the Rh6G (0.25 mM) doped POF [Fig. 7(a)], 595.4–605.1 nm for the Rh6G (0.25 mM) and RhB (0.11 mM) doped POF [Fig. 7(b)], 599.5–609.1 for the Rh6G (0.25 mM) and RhB (0.25 mM) doped POF [Fig. 7(c)], and 600.5–608.6 nm for the RhB (0.25 mM) doped POF [Fig. 7(d)]. The second peak does not show any considerable peak shift. The observed redshift of the first peak is due to the self-absorption and reemission process (radiative energy transfer) taking place within the dye doped fiber as the propagation distance increases (case 2). The reabsorption process occurs only at the shorter wavelength part of the fluorescence signal. Therefore no redshift is observed for the second peak at the longer wavelength part in the case of Figs. 6(b)–6(d).

It should be noted here that in the case of the dye mixture doped samples in Figs. 6(b) and 6(c), the propagating fluorescence light gets absorbed only by the RhB molecule, and there is hardly any chance of absorption by the Rh6G molecule. As is obvious from the absorption spectrum (Fig. 2), the absorption band of the Rh6G ends at 570 nm, and the fluorescence light from the dye mixture system is beyond that wavelength.

3. A clear energy transfer occurs from the first peak region of the fluorescence spectrum to the second peak region in the case of Figs. 6(b)–6(d) as the propagation distance is increased from 4 to 26 mm. To obtain a clear picture of this energy trans-

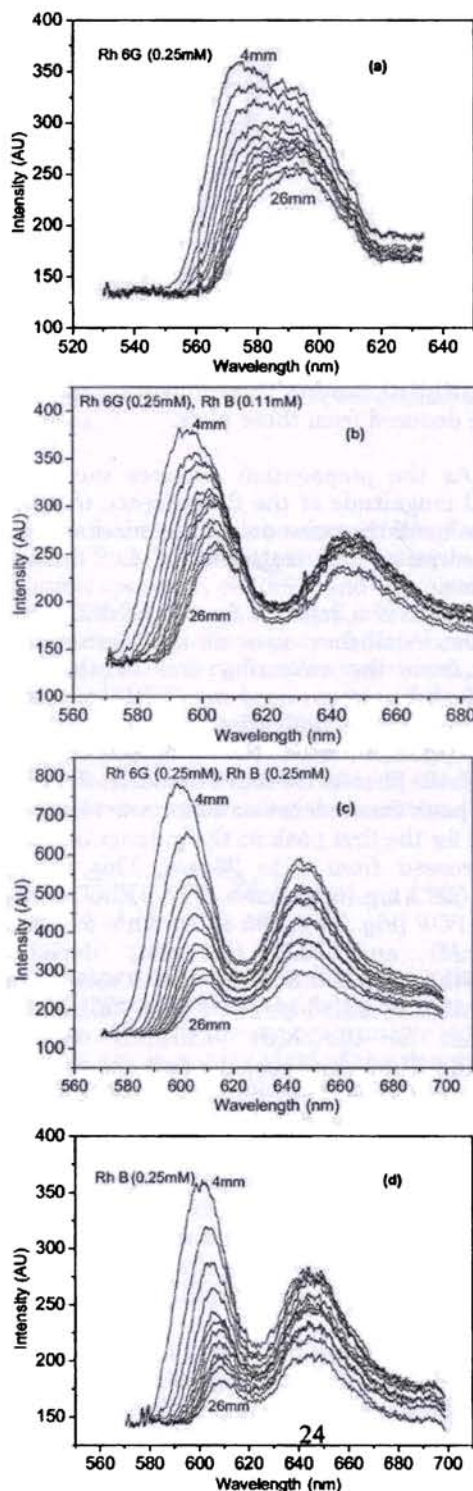


Fig. 6. TPE SIF spectra for different propagation distances (4–26 mm) through the fiber; (a) Rh6G (0.25 mM), (b) dye mixture Rh6G (0.25 mM) and RhB (0.11 mM), (c) dye mixture Rh6G (0.25 mM) and RhB (0.25 mM), and (d) RhB (0.25 mM).

fer, the intensity ratio of the first peak with respect to the second peak (I_1/I_2) versus the propagation distance is plotted in the case of the last three fiber sam-

ples in Figs. 6(b)–6(d) [Fig. 8(a)]. In all three of the plots (I_1/I_2) decrease with the propagation distance. The decrease in the value of intensity ratio is a clear indication of the existence of an energy transfer from the first peak to the second peak. As mentioned earlier, the shorter wavelength part of the fluorescence spectrum corresponding to the first peak gets self-absorbed by the RhB molecule and is reemitted at a longer wavelength as the propagation distance is increased. This causes relatively more loss at the first peak region and a net gain at the second peak region. Thus, in effect, energy transfer of a radiative type occurs from the first peak region to the second peak region of the fluorescence spectrum as the propagation distance increases.

Considering the case of the samples in Figs. 6(c) and 6(d), the energy transfer effect is almost at the same rate as a result of the equal RhB concentration (0.25 mM) in both cases. For the Rh6G (0.25 mM) and RhB (0.11 mM) doped sample, the effect is less prominent as expected because of the lower RhB concentration, which is the main component of this energy transfer process.

We can define a transfer coefficient, β , which can be deduced from the $\ln(I_1/I_2)$ versus distance plot [Fig. 8(b)] such that

$$Y(z) = Y_{(0)}e^{-\beta z} \quad (3)$$

where $Y = I_1/I_2$, $Y(z)$ is the intensity ratio value after a propagation distance z , $Y_{(0)}$ is the initial intensity ratio value, and β is the transfer coefficient.

It is observed that the plots in Fig. 8(b) cannot be fitted to a single straight line, but it can be peeled off to two straight lines using the peeling curve method [41,42] corresponding to two transfer coefficients β_1 and β_2 such that

$$Y(z) = Y_{(01)}e^{-\beta_1 z} \quad (4)$$

for shorter propagation distances,

$$Y(z) = Y_{(02)}e^{-\beta_2 z} \quad (5)$$

for longer propagation distances.

The above equations can be expressed as

$$Y(z) = Y_{01}H(Z_c - Z)e^{-\beta_1 z} + Y_{02}H(Z - Z_c)e^{-\beta_2 z}, \quad (6)$$

where $H(x)$ is the Heaviside step function such that

$$H(x) = 1, \quad x > 0 = 0, \quad x < 0.$$

Z_c is a critical length below which the intensity ratio varies according to the first component in Eq. (6) with the energy transfer coefficient β_1 and above which it varies according to the second component with the energy transfer coefficient β_2 .

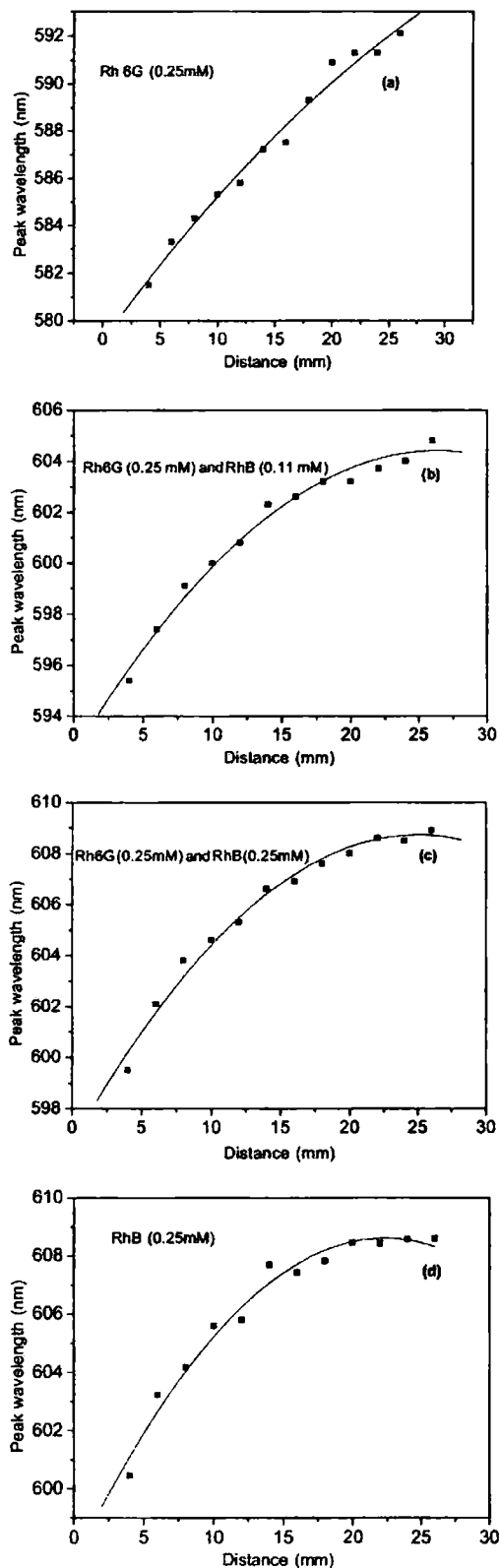


Fig. 7. Redshift of the peak fluorescence emission with propagation distance (4–26 mm) through the fiber. (a) Rh6G (0.25 mM), (b) dye mixture Rh6G (0.25 mM) and RhB (0.11 mM), (c) dye mixture Rh6G (0.25 mM) and RhB (0.25 mM), and (d) RhB (0.25 mM).

It is observed that the transfer coefficient values obtained from the slopes of the peeled off straight lines for shorter propagation distances β_1 are higher than the longer propagation distance value β_2 in all three cases. Therefore it is evident that the energy transfer is greater at shorter propagation distances, and it saturates at longer propagation distances. As the propagation distance increases the fluorescence spectrum shows a redshift as shown in Fig. 6. As a result, the extent of spectral overlap between the absorption and the fluorescence emission, which is the main cause of this energy transfer process, goes on decreasing as the propagation distance increases. This decrease in the extent of spectral overlap causes the reduction in the energy transfer process at longer propagation distances compared to shorter propagation distances.

In the case of the RhB doped POF, the transfer coefficient value obtained from the slopes of the peeled off straight lines for shorter propagation distances, β_1 is 0.033, which is higher than the value of 0.003 for longer propagation distances and a similar behavior is observed for the other two samples in Figs. 6(b) and 6(c). Again, the transfer coefficient ($\beta_1=0.016$) for the Rh6G (0.25 mM) and RhB (0.11 mM) doped POF is lower than the corresponding transfer coefficient $\beta_1=0.041$ for the Rh6G (0.25 mM) and RhB (0.25 mM) doped POF as expected because of the lesser number of RhB molecules and hence less energy transfer.

C. Attenuation Coefficient

Fluorescence emission collected from the dye doped fiber has a spectral width of ~ 100 nm, and that itself can be used as a broad-wavelength light source to characterize the attenuation coefficient in the dye doped POF. The transmitted fluorescence is measured as a function of propagation distance so as to characterize the attenuation in the fiber.

From Beer–Lambert’s law for a linear optical attenuation in a medium

$$I(\lambda, z) = I_0(\lambda) \exp(-\alpha(\lambda)z), \quad (7)$$

where $I(\lambda, z)$ and $I_0(\lambda)$ represent the intensity of the transmitted light at wavelength λ for propagation distances z and $z = 0$, respectively, and $\alpha(\lambda)$ is the linear attenuation coefficient.

Figure 9 shows the natural logarithm of the transmitted intensity versus the propagation distance (data taken from Fig. 6) for different wavelengths in the case of the above-mentioned four samples. An interesting observation is the nonlinear behavior of the $\ln I$ versus distance plot, which suggests that the attenuation coefficient is not a constant for the total length of propagation through the fiber. The nonlinear plot of $\ln I$ versus z can be fitted to a minimum number of straight lines, which will provide the corresponding attenuation coefficients [41,42]. The plots can be peeled off to two straight lines corresponding to two different attenuation coefficients

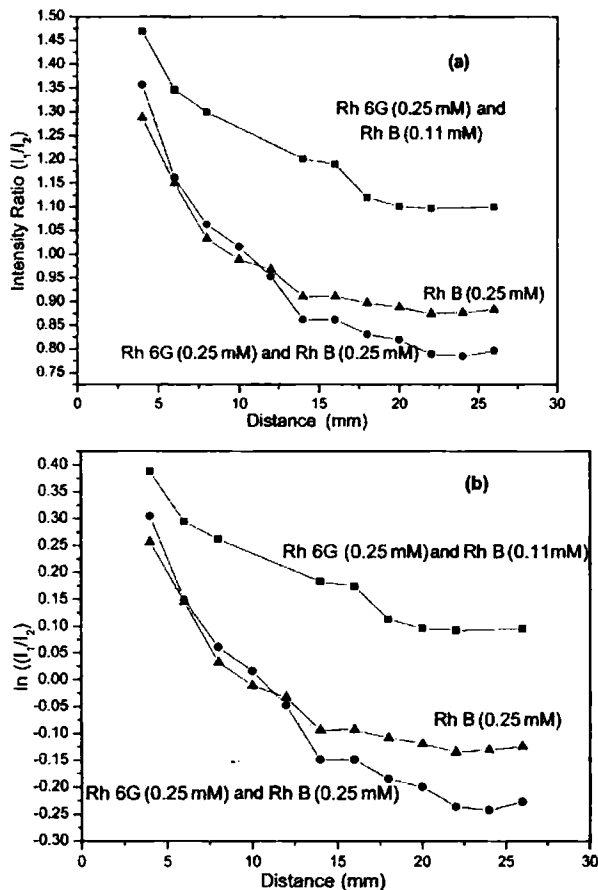


Fig. 8. (a) Intensity ratio of the first peak with respect to the second peak (I_1/I_2) versus the propagation distance. (b) Natural logarithm of (I_1/I_2) versus the propagation distance.

α_1 and α_2 for shorter and longer propagation distances, respectively.

The spatial dependence of intensity variation along the length of the fiber can be represented by the following equation using the Heaviside step function:

$$I_z = I_{01}H(Z_0 - Z)e^{-\alpha_1 z}I_{02}H(Z - Z_0)e^{-\alpha_2 z}, \quad (8)$$

where Z_0 is a critical length below which the intensity decreases according to the first component in Eq. (8) with the attenuation coefficient α_1 and above that according to the second component with the attenuation coefficient α_2 .

It is observed that there is a decrease in the attenuation coefficient for longer propagation distances compared to shorter propagation distances in all four cases corresponding to the first peak wavelengths (say 560, 570, 580, 590, 600 etc.). This is due to the reabsorption and reemission effects observed in the dye molecules as the propagation distance is increased. As the propagation distance increases, the propagating light interacts with a higher number of dye molecules, which results in enhanced emission and thereby a reduction in loss. This result is in accordance with the higher transfer

coefficient β_1 at shorter propagation distances, which leads to the increase in the attenuation coefficient at shorter distances compared to longer propagation distances.

When a short distance of propagation is considered, the attenuation coefficient is found to be larger for shorter wavelengths compared to longer wavelengths in all the samples. The reabsorption of propagating fluorescence light by dye molecules is more at the shorter wavelength side of the fluorescent emission spectrum due to the overlap between the absorption spectrum and shorter wavelength part of the fluorescent spectrum of dye molecules. This reabsorbed light gets emitted at a longer wavelength. So the emission intensity at the longer wavelength side is larger, and attenuation is less compared to the shorter wavelength region.

The attenuation coefficient for wavelengths (say 640, 645, 650 nm) in the second peak region is found to be much less compared to the attenuation at shorter wavelengths in the first peak region [Figs. 9(b)–9(d)]. This is because of the energy gain achieved by the second peak region due to the energy transfer occurring from the first peak to the second peak.

Another observation is that the attenuation coefficient for the wavelengths in the second peak region is found to be slightly lower at shorter propagation distances than at longer distances. This is in accordance with the result that β , the transfer coefficient, is higher at shorter propagation distances than at longer distances. This results in a maximum energy transfer leading to a reduction in loss at shorter propagation distances for the second peak region.

4. Conclusions

TPE SIF spectrum from a Rh6G:–RhB dye mixture doped POF was found to be redshifted compared to that of a Rh6G doped POF due to the energy transfer occurring from Rh6G to RhB. The Forster distance in the Rh6G–RhB dye mixture system is found to be 55 Å, indicating that FRET can also be a mechanism of energy transfer along with the radiative type. The fluorescence intensity of a RhB doped POF gets enhanced in the presence of Rh6G as a result of this energy transfer. Position dependent tuning of TPE SIF spectra have been observed for different dye mixture doped POF samples. As a result of the reabsorption and reemission process in dye molecules, an effective energy transfer is observed from the shorter wavelength part of the fluorescence spectrum to the longer wavelength part as the propagation distance is increased in the dye doped POF. The energy transfer coefficient is found to be higher at shorter propagation distances compared to longer distances. The TPE fluorescence signal is used to characterize the optical attenuation coefficient in a dye doped POF. The attenuation coefficient is lower at longer propagation distances compared to shorter distances. This is due to the reabsorption and reemission process taking place within the dye doped fiber as the propagation distance is increased. The attenuation coeffi-

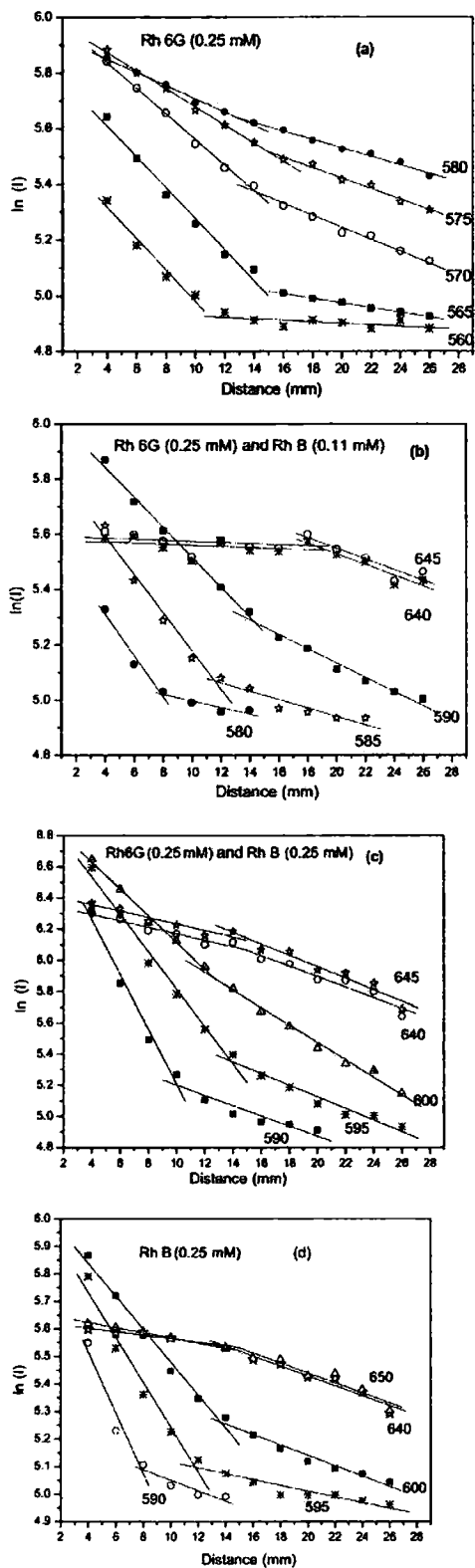


Fig. 9. Natural logarithm of the transmitted intensity versus the propagation distance through the fiber for different wavelengths. (a) Rh6G (0.25 mM), (b) dye mixture Rh6G (0.25 mM) and RhB (0.11 mM), (c) dye mixture Rh6G (0.25 mM) and RhB (0.25 mM), and (d) RhB (0.25 mM).

cient is found to be larger for shorter wavelengths compared to longer wavelengths due to the enhanced reabsorption of fluorescent light at the shorter wavelength side. The attenuation coefficient for wavelengths in the second peak region is found to be much less compared to the loss at the shorter wavelength in the first peak region due to the energy gain achieved in the second peak. These results on energy transfer and the attenuation coefficient are useful for the appropriate selection of specific combinations of dyes for efficient upconverted lasing in a dye doped POF.

The authors acknowledge financial support from the Centre of Excellence in Lasers and Optoelectronic Sciences, Cochin University of Science and Technology. M. Sheeba thanks the University Grants Commission, New Delhi, for the research fellowship.

References

1. Y. Koike, T. Ishigure, and E. Nihei, "Highbandwidth graded-index polymer optical fiber," *J. Lightwave Technol.* **13**, 1475–1489 (1995).
2. M. A. van Eijkelenborg, A. Argyros, G. Barton, I. M. Bassett, M. Fellet, G. Henry, N. A. Issa, M. C. J. Large, S. Manos, W. Padden, L. Poladian, and J. Zagari, "Recent progress in microstructured polymer optical fibre fabrication and characterization," *Opt. Fiber Technol.* **9**, 199–209 (2003).
3. F. M. Cox, A. Argyros, and M. C. J. Large, "Liquid-filled hollow core microstructured polymer optical fiber," *Opt. Express* **14**, 4135–4140 (2006).
4. M. R. Sheeba, K. Geetha, C. P. G. Vallabhan, P. Radhakrishnan, and V. P. N. Nampoori, "Fabrication and characterization of dye doped polymer optical fiber as a light amplifier," *Appl. Opt.* **46**, 106–112 (2007).
5. K. Kuriki, T. Kobayashi, N. Imai, T. Tamura, S. Nishihara, Y. Nishizawa, A. Tagaya, and Y. Koike, "High efficiency organic dye doped polymer optical fiber lasers," *Appl. Phys. Lett.* **77**, 331–333 (2000).
6. R. Gvishi, G. Ruland, and P. N. Prasad, "New laser medium: dye-doped sol-gel fiber," *Opt. Commun.* **126**, 66–72 (1996).
7. S. Muto, A. Ando, O. Yoda, T. Hanawa, and H. Ito, "Tunable laser by sheet of dye doped plastic fibers," *Trans. Inst. Electron. Inf. Commun. Eng. J70-C*, 1479–1484 (1987).
8. M. Kuwata-Gonokami, R. H. Jordan, A. Dodabalapur, H. E. Katz, M. L. Schilling, R. E. Slusher, and S. Ozawa, "Polymer microdisc and microring lasers," *Opt. Lett.* **20**, 2093–2095 (1995).
9. A. Otomo, S. Yokoyama, T. Nakahama, and S. Mashiko, "Super narrowing mirrorless laser emission in dendrimer doped polymer waveguides," *Appl. Phys. Lett.* **77**, 3881–3883 (2000).
10. K. Svoboda and R. Yasuda, "Principles of two-photon excitation microscopy and its applications to neuroscience," *Neuron* **50**, 823–839 (2006).
11. E. Heumann, S. Bar, K. Rademaker, G. Huber, S. Butterworth, A. Diening, and W. Seelert, "Semiconductor-laser-pumped high-power upconversion laser," *Appl. Phys. Lett.* **88**, 061108 (2006).
12. G. Qin, S. Huang, Y. Feng, A. Shirakawa, M. Musha, and K. I. Ueda, "Power scaling of Tm^{3+} doped ZBLAN blue upconversion fiber lasers: modeling and experiments," *Appl. Phys. B* **82**, 65–70 (2006).
13. M. Goppert-Mayer, "Ueber elementarakte mit zwei quanen-sprengen," *Ann. Phys.* **9**, 273–294 (1931).
14. W. K. Kaiser and C. G. B. Garrett, "Two-photon excitation in $CaF_2:Eu^{2+}$," *Phys. Rev. Lett.* **7**, 229–231 (1961).

15. X. H. Yang, J. M. Hays, W. Shan, and J. J. Song, "Two-photon pumped blue lasing in bulk ZnSe and ZnSSe," *Appl. Phys. Lett.* **62**, 1071–1073 (1993).
16. G. S. He, L. Yuan, P. N. Prasad, A. Abbotto, A. Facchetti, and G. A. Pagani, "Two photon pumped frequency upconversion lasing of a new blue green dye material," *Opt. Commun.* **140**, 49–52 (1997).
17. A. S. Kwok, A. Serpenguzel, W. F. Hsieh, and R. K. Chang, "Two-photon-pumped lasing in microdroplets," *Opt. Lett.* **17**, 1435–1437 (1992).
18. G. S. He, C. F. Zhao, J. D. Bhawalkar, and P. N. Prasad, "Two-photon pumped cavity lasing in novel dye doped bulk matrix rods," *Appl. Phys. Lett.* **67**, 3703–3705 (1995).
19. G. S. He, J. D. Bhawalkar, C. F. Zhao, C. K. Park, and P. N. Prasad, "Upconversion dye-doped polymer fiber laser," *Appl. Phys. Lett.* **68**, 3549–3551 (1996).
20. A. Mukherjee, "Two photon pumped upconverted lasing in dye doped polymer waveguides," *Appl. Phys. Lett.* **62**, 3423–3425 (1993).
21. D. C. Nguyen, G. E. Faulkner, and M. Dulick, "Blue-green (450 nm) upconversion Tm³⁺:YLF laser," *Appl. Opt.* **28**, 3553–3555 (1989).
22. Y. Mita, Y. Wang, and S. Shionoya, "High brightness blue and green light sources pumped with a 980 nm emitting laser diode," *Appl. Phys. Lett.* **62**, 802–804 (1993).
23. D. W. Garwey, K. Zimmerman, P. Young, J. Tostenrude, J. S. Townsend, Z. Zhou, M. Lobel, M. Dayton, R. Wittorf, and M. G. Kuzyk, "Single mode nonlinear optical polymer fibers," *J. Opt. Soc. Am. B* **13**, 2017–2023 (1996).
24. T. Kaino, "Waveguide fabrication using organic nonlinear optical materials," *J. Opt. A, Pure Appl. Opt.* **2**, R1–R7 (2000).
25. R. J. Kruhlak and M. G. Kuzyk, "Side-illumination fluorescence spectroscopy. I. Principles," *J. Opt. Soc. Am. B* **16**, 1749–1755 (1999).
26. R. J. Kruhlak and M. G. Kuzyk, "Side-illumination fluorescence spectroscopy. II. Applications to squaraine dye-doped polymer optical fibers," *J. Opt. Soc. Am. B* **16**, 1756–1767 (1999).
27. M. Sheeba, K. J. Thomas, M. Rajesh, V. P. N. Nampoori, C. P. G. Vallabhan, and P. Radhakrishnan, "Multimode laser emission from dye doped polymer optical fiber," *Appl. Opt.* **46**, 8089–8094 (2007).
28. C. Xu and W. W. Webb, "Measurement of two photon excitation cross sections of molecular fluorophores with data from 690 to 1050 nm," *J. Opt. Soc. Am. B* **13**, 481–491 (1996).
29. G. A. Kumar, V. Thomas, G. Thomas, N. V. Unnikrishnan, and V. P. N. Nampoori, "Energy Transfer in Rh 6G: Rh B system in PMMA matrix under CW laser excitation," *J. Photochem. Photobiol. A* **153**, 145–151 (2002).
30. N. V. Unnikrishnan, H. S. Bhatti, and R. D. Singh, "Energy transfer in dye mixtures studied by laser fluorimetry," *J. Mod. Opt.* **31**, 983–987 (1984).
31. J. R. Lakowicz, *Principles of Fluorescence Spectroscopy* (Springer, 2006), p. 445.
32. D. Seth, D. Chakrabarty, A. Chakraborty, and N. Sarkar, "Study of energy transfer from 7-amino coumarin donors to rhodamine 6G acceptor in non-aqueous reverse micelles," *Chem. Phys. Lett.* **401**, 546–552 (2005).
33. C. h. Scharf, K. Peter, P. Bauer, Ch. Jung, M. Thelakkat, and J. Kohler, "Towards the characterisation of energy-transfer processes in organic donor-acceptor dyads based on triphenylidamine and perylenebisimides," *Chem. Phys.* **328**, 403–409 (2006).
34. G. Cerulla, S. Stagira, M. Zavelani-Rossi, S. D. Silvestri, T. Virgili, D. G. Lidzey, and D. D. C. Bradley, "Ultrafast Forster transfer dynamics in tetraphenylporphyrin doped poly(9,9-dioctylfluorene)," *Chem. Phys. Lett.* **335**, 27–33 (2001).
35. A. V. Deshpande and E. B. Namdas, "Correlation between lasing and photo physical performance of dyes in polymethylmethacrylate," *J. Lumin.* **91**, 25–31 (2000).
36. J. Brandrup, E. H. Immergut, and E. S. Grulke, "Refractive indices of polymers" in *Polymer Handbook*, 4th ed. (Wiley, 1999), Vol. 1, p. 571.
37. P. R. Selvin, "The renaissance of fluorescence resonance energy transfer," *Nat. Struct. Biol.* **7**, 730–734 (2000).
38. J. N. Miller, "Fluorescence energy transfer methods in bioanalysis," *Analyst (Amsterdam)* **130**, 265–270 (2005).
39. R. D. Singh, A. K. Sharma, N. V. Unnikrishnan, and D. Mahan, "Energy transfer study on Coumarin 30-Rhodamine 6G dye mixture using a laser fluorimeter," *J. Mod. Opt.* **37**, 419–425 (1990).
40. P. J. Sebastian and K. Sathianandan, "Donor concentration dependence of the emission peak in rhodamine 6G-rhodamine B energy transfer dye laser," *Opt. Commun.* **35**, 113–114 (1980).
41. M. Rajesh, K. Geetha, M. Sheeba, C. P. G. Vallabhan, P. Radhakrishnan, and V. P. N. Nampoori, "Characterisation of rhodamine 6G doped polymer optical fiber by side illumination fluorescence," *Opt. Eng.* **45**, 075003 (2006).
42. K. Geetha, M. Rajesh, V. P. N. Nampoori, C. P. G. Vallabhan, and P. Radhakrishnan, "Loss characterisation in rhodamine 6G doped polymer film waveguide by side illumination fluorescence," *J. Opt. A Pure. Appl. Opt.* **6**, 379–383 (2004).